SACLANTCEN REPORT
serial no: SR- 335

SACLANT UNDERSEA RESEARCH CENTRE REPORT

NORTH ATLANTIC TREATY ORGANIZATION ORGANISATION DU TRAITE DE L'ATLANTIQUE NORD

Normal incidence reflection loss from a sandy sediment

N.P. Chotiros, A. P. Lyons, J. Osler and N.G. Pace

The content of this document pertains to work performed under Project 03-D of the SACLANTCEN Programme of Work. The document has been approved for release by The Director, SACLANTCEN.

Jan L. Spoelstra
Director

intentionally blank page

Normal incidence reflection loss from a sandy sediment

N.P. Chotiros*, A. P. Lyons, J. Osler and N.G. Pace

Executive Summary:

The detection of mines buried in the seabed is of continuing concern. The optimization of sonars for such purposes depends critically on the understanding of the interactions of acoustics with the seabed. A well advertized limitation to search geometries is the existence of a critical angle for the incidence of an acoustic wave on the seabed. Beyond this angle most of the acoustic energy is reflected back into the water. In practice, this limitation is ill-defined because of small scale sediment variability and water-sediment interface roughness. There have been a number of experimental and theoretical attempts to further understand the nature of the critical angle limitation. There are models of varying complexity, which may be used to describe the acoustic properties of the sediment. This report provides, through the analysis of a simple normal incidence experiment, evidence to support the appropriateness of one model over another.

*Applied Research Laboratory, Univ. of Texas, Austin, TX 78713, U.S.A.

intentionally blank page

Normal incidence reflection loss from a sandy sediment

N.P. Chotiros, A. P. Lyons, J. Osler and N.G. Pace

Abstract:

Acoustic reflection loss at normal incidence of a sandy sediment, in the Biodola Gulf on the north side of the island of Elba, Italy, was measured in the band 8 - 17 kHz, using a self-calibrating method. The water depth was approximately 11 m the sand pure with a mean grain diameter of 0.2 mm. The measured reflection loss 11 dB, ±2 dB is consistent with measurements in the published literature. The computed reflection loss for an interface between water and a uniform visco-elastic media with the same properties was 8 dB, ±1dB. The theoretical and experimental values do not significantly overlap, which leads to the conclusion that the visco-elastic model is inappropriate. The Biot model is suggested as a better alternative but more work is needed to ascertain the appropriate parameter values.

Keywords: Acoustic reflection loss - Biot model - seafloor sediments

Contents

1
Introduction

Normal incidence reflection of sound from ocean sediments is relatively easy to detect. It is used in depth-sounders to give water depth measurements. Mariners and fishermen have observed that the signature of the bottom echo changes with location and some have claimed to be able to interpret them in various ways. Yet, there has been little experimentation and verification of acoustic models with respect to the reflection loss. Some have assumed that the ocean sediment behaves like an elastic medium and proceeded to use reflection measurements to invert for sediment properties [1], or to use sediment properties to predict reflection loss [2], with varying degrees of success. It will be shown in this study that the elastic medium assumption is inadequate for sandy ocean sediments. As sand is a porous medium rather than a uniform elastic solid, Biot's model [3] of sound propagation in a porous elastic medium is likely to be a better alternative. Using Biot's theory as formulated by Stoll and Kan [4], it is possible to compute the reflection coefficient given the relevant input parameters. The disadvantage of the Biot model is that it requires a large number of input parameters, some of which are difficult to measure.

The scope of this study is limited to the measurement of the normal incidence reflection loss over sandy sediments and a comparison of the results to elastic media theory. This comparison is complicated by the roughness of the sand surface. The theoretically computed reflection loss is applicable to a flat surface of infinite extent but the sand surface at the experimental site is not flat. Numerical examples have been computed for a sand surface with a roughness spectrum similar to the surface at the experimental site, particularly the 0.2 m ripple wavelength [5]. With regard to the possibility of relating the measured reflection loss of a rough surface to that of a flat surface, there are two factors. (1) The Kirchhoff approximation is necessary to make the connection between rough and flat surfaces. It was concluded from the numerical simulations that the Kirchhoff approximation is valid above 10 kHz. (2) The surface roughness randomizes the reflected signal, necessitating a statistical approach. The signal intensity, averaged over several pings, is a possible statistic. Numerical modelling showed a reduction in the peak value of the average reflected intensity, relative to that of a flat surface, due to time spreading of the acoustic energy by the roughness scattering, that increased with both height above the sand and signal frequency. Interpolating from the numerical results to a height above bottom appropriate to this experiment, the estimated reduction is less than 2 dB, for frequencies below 20 kHz. The reduction due to time spreading may be overcome by integrating the average signal intensity over a window that contains the significant part of the reflected and scattered energies. Using a wide-beam receiver to capture the energy over all significant scattering angles, this statistic is a reliable measure of the reflection loss. The numerical simulations also indicated that the volume scattering component, due

to inhomogeneities within the sand, would be insignificant compared to that of the surface reflection and scattering.

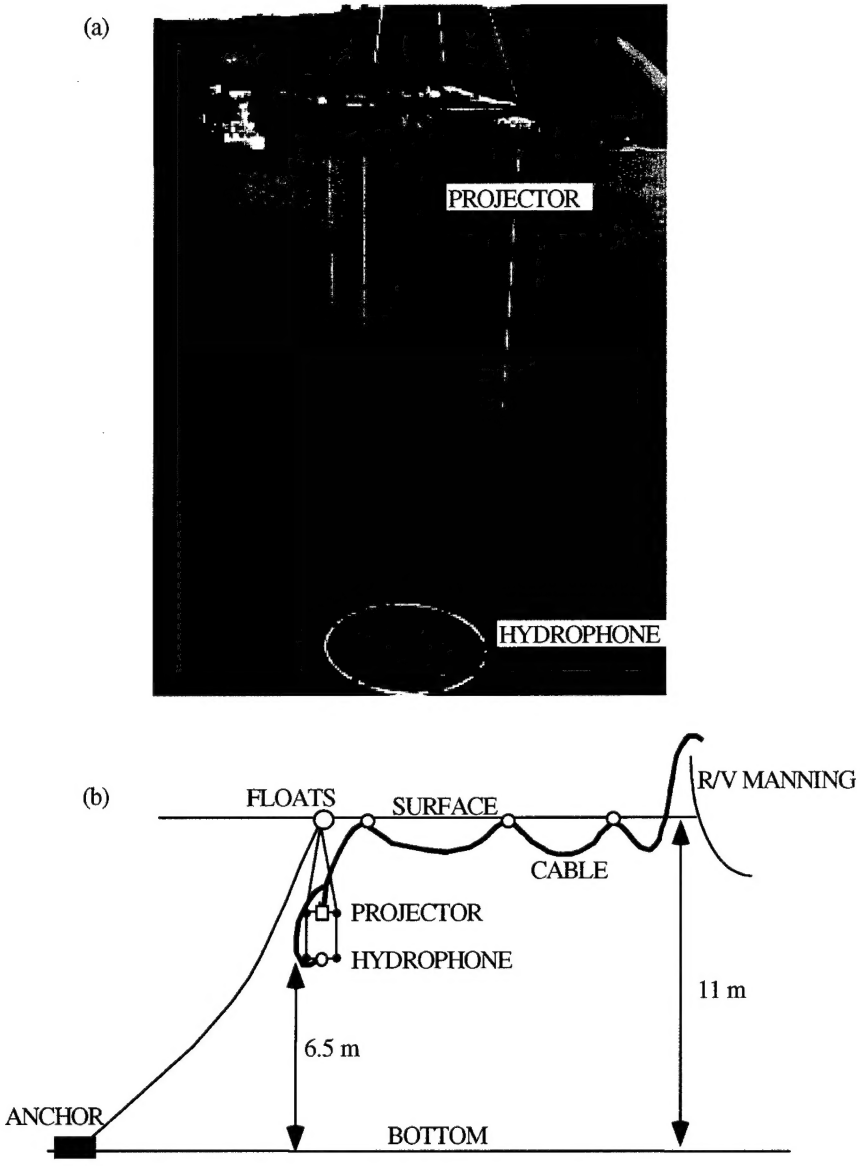

Figure 1 *(a) Photograph of projector and hydrophone assembly and (b) diagram of deployment over the sediment.*

Surface conditions were calm throughout the experiment. The site was in a relatively sheltered bay. There was only a small amount of source motion induced by wave activity, mainly in the vertical direction. Consequently, changes in source angle were small. Given the wide source beam width, changes in the bottom insonification would have been a

very small fraction of a decibel. This is confirmed by the almost imperceptible variation from one ping to the next of the direct path signal from projector to hydrophone.

The choice of source and hydrophone depths was dictated by a number of considerations. The source had to be sufficiently removed from the surface so that the surface bounce signal would not interfere with the direct arrival at the hydrophone. The projector to hydrophone separation (ph) had to be greater than the Rayleigh distance of the source, which is estimated to be less than a metre at 20 kHz. The bottom reflection (pbh) must be sufficiently separated in time from the surface reflection (psh) as well as the surface-bottom multiples (psbh, pbsh). The expected arrival times of the various signals are shown in Fig. 2.

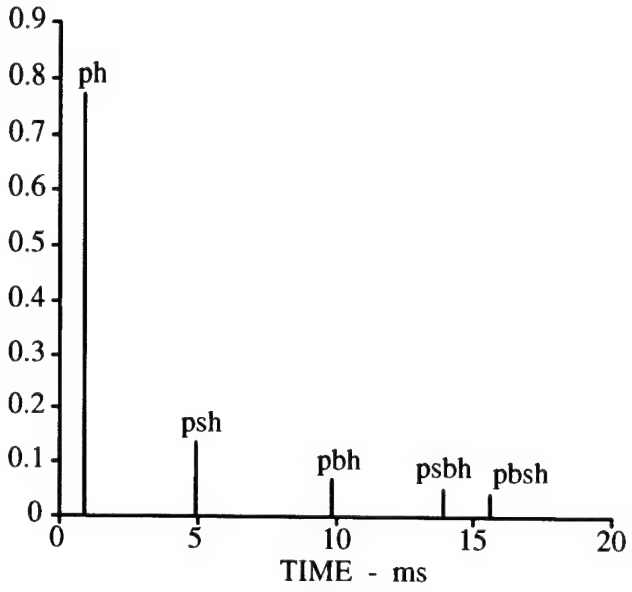

Figure 2 *Expected arrival times of various signal paths.*

The projected signal was a gated sine-wave of exactly three cycles. This was a compromise, found by experimentation, which provided a workable balance between the need to maximize signal pulse length to obtain a high signal-to-noise ratio after filtering and the need to limit the pulse length to allow the multiple arrivals to be separable in time. With the given source transducer, it was found that a pulse shorter than 3 cycles caused excessive ringing and did not carry enough energy. In order to cover the band from 10 to 20 kHz, it was determined that 3 cycle pulses at 2 kHz intervals would provide adequate coverage. The amplifier gain had to be adjusted so that the direct path signal did not saturate the system and yet allow the bottom-reflected signal to be clearly measurable above the background noise. An example of a received raw signal is shown in Fig. 3; the plot axes scales were adjusted to show the bottom and other reflected signals and not the direct signal from the projector. The projector to hydrophone (ph) and the bottom bounce

(pbh) signals could be separated by time gating. In both cases, a window length of 4 ms was found to be adequate. In addition to the acoustic signals, there were a couple of electrical pulses: the feed-over from the projector power amplifier (e1) and a timing pulse (e2). Both e1 and e2 are electrical cross-talk that normally occur in experiments of this nature. They occur at definite time intervals after pulse transmission and they are completely separable by time gating from the desired acoustic signals. Expanded views of the windowed signals are shown in Figs. 4 and 5. The dynamic range was between + and – 10 volts with 16-bit resolution. The direct path signal was safely within these limits and, although the bottom reflection was considerably weaker, it was clearly measurable.

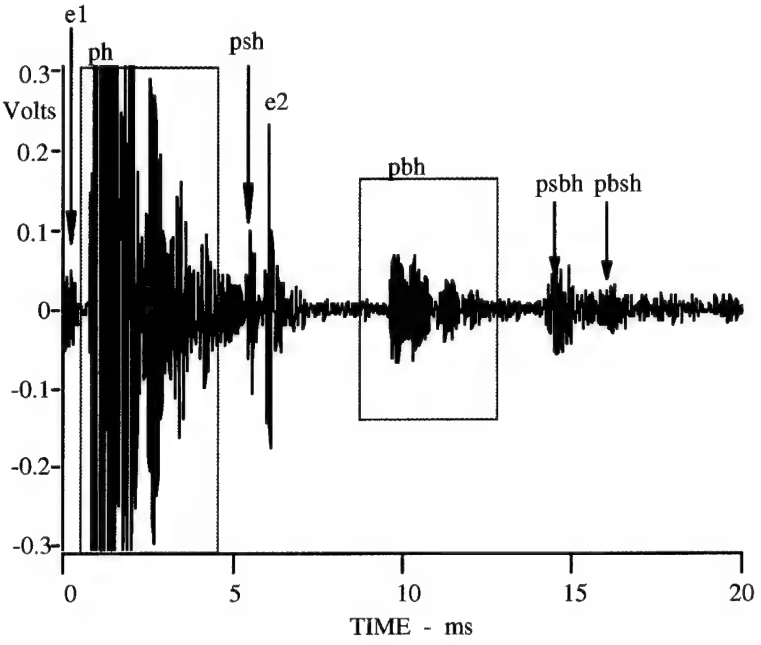

Figure 3 *Example of raw signal measured at the hydrophone.*

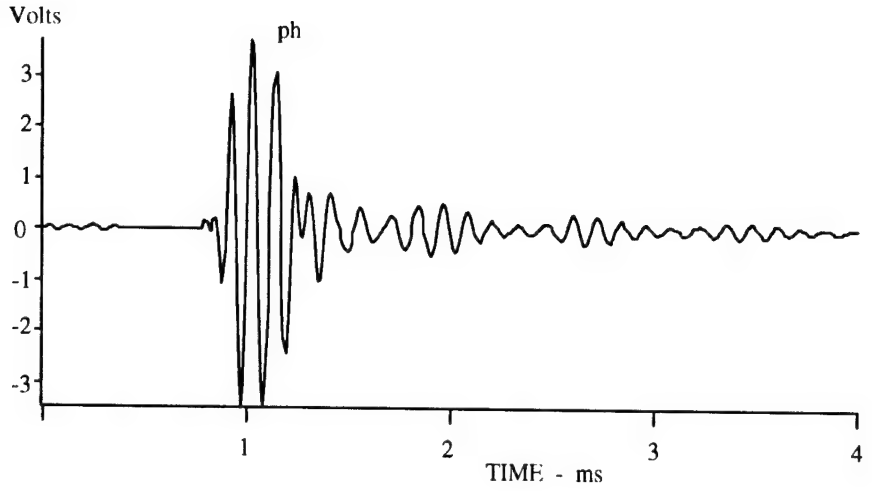

Figure 4 *Expanded view of a direct path signal.*

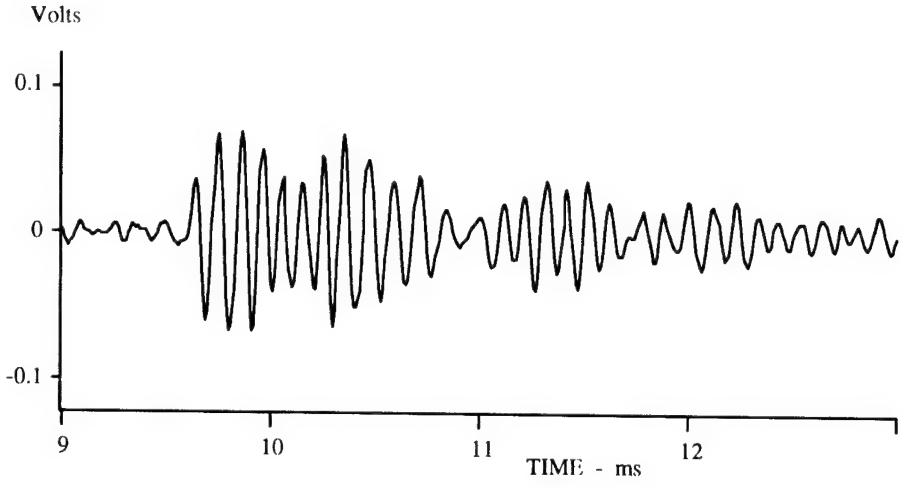

Figure 5 *Expanded view of a raw bottom reflected pulse.*

On a ping to ping basis, the bottom reflection was a random process, because the projector and hydrophone were constantly in motion about their equilibrium positions under the influence of the waves and currents and because the bottom was not a perfectly flat surface. The water-sediment interface was dominated by ripples of the order of a centimetre in amplitude and by mounds caused by biological activity, as shown in the photograph in Fig. 6.

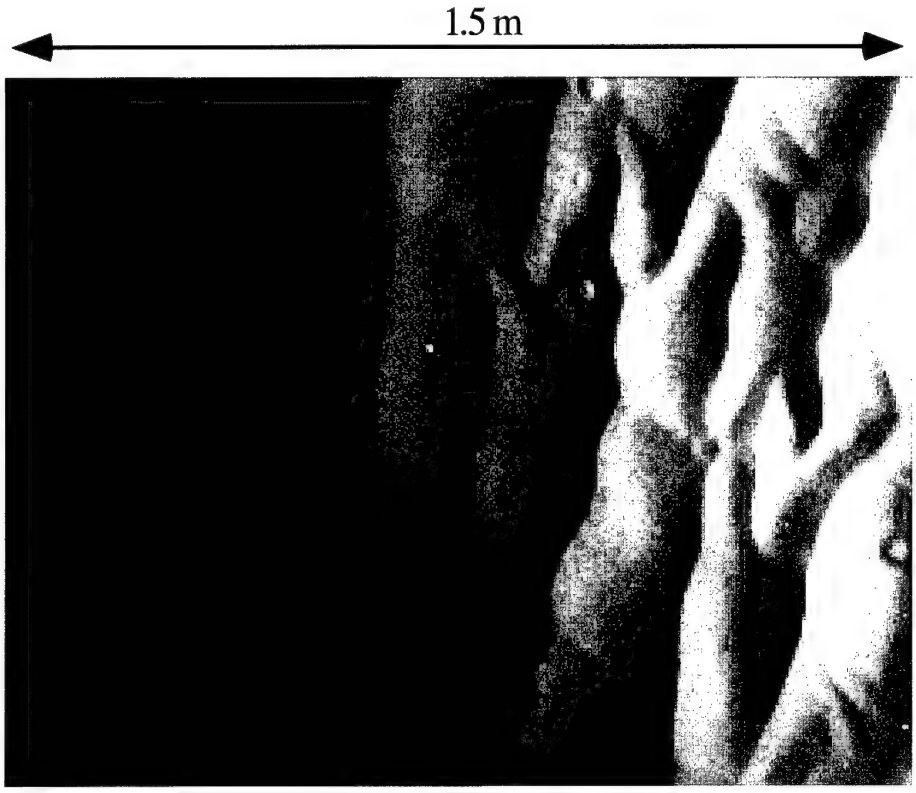

Figure 6 *A photograph of the sediment.*

Data were recorded at carrier frequencies 9, 11, 13, 15, 17 and 19 kHz. At each frequency, 1000 pings were recorded, at a rate of 2 pings per second. This was necessary because the reflected signal is a random process and a large number of pings were needed in order to obtain accurate statistics. An example of the average intensity, in decibels, as a function of time, computed from a set of 250 pings, is shown in Fig. 7. The direct (ph) and bottom reflected (pbh) signals are clearly detectable and separable from the electrical interferences (e1, e2) and the other acoustic arrivals, including the surface reflection (psh) and the surface-bottom multiples (psbh, pbsh).

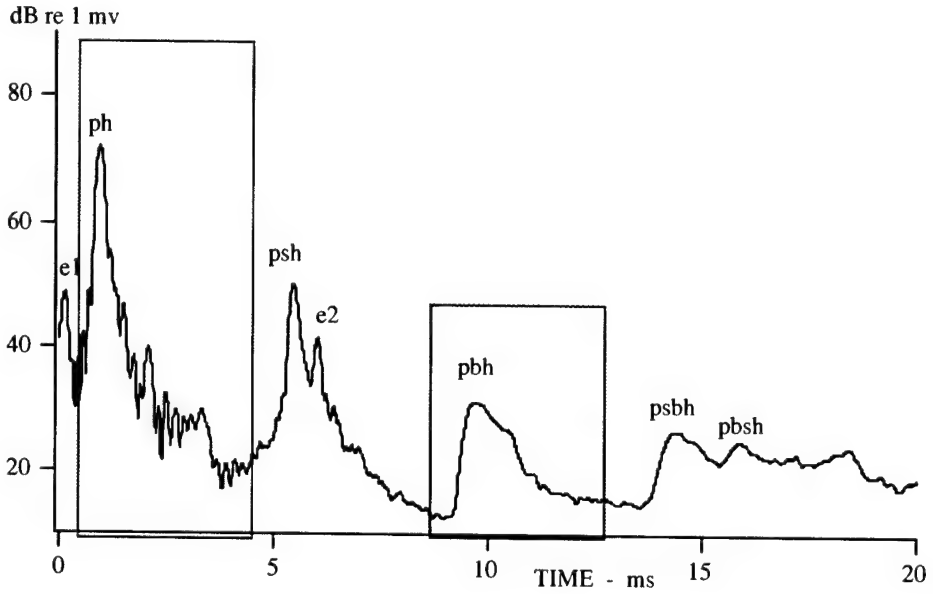

Figure 7 *Average intensity from a set of 250 pings.*

3
Screening

At each centre frequency, the 1000 pings were divided into 4 sets of 250 pings. The averaged signal intensity of each set was compared to the other three. Assuming Rayleigh statistics, the average of 250 pings would have a standard error of 6.3% or 0.27 dB. Therefore, the set averages should agree to within a small fraction of a decibel. Some anomalies were found. In the 19 kHz data, (Fig. 8), sets 2, 3 and 4 were mutually consistent, but set 1 had an anomalously large decay tail, possibly due to a school of fish or because the equipment drifted too close to a patch of seagrass known to be at the periphery of the experimental area. Another example is shown in Fig. 9, in which only sets 1 and 2 of the 13 kHz data were mutually consistent. Sets 3 and 4 appear to have additional scattered energy before and after the main bottom reflected signal, possibly due to a school of fish passing beneath the transducers. It was determined that, out of 4 sets, 2 or more mutually consistent sets would be acceptable. The 2 or more mutually consistent sets would be accepted and the others rejected. A summary of the screening results is shown in Table I. The data set obtained at a centre frequency of 17 kHz was completely rejected because there was very little mutual consistency between the four sets. The accepted data sets were used in the subsequent processing to compute the reflection loss.

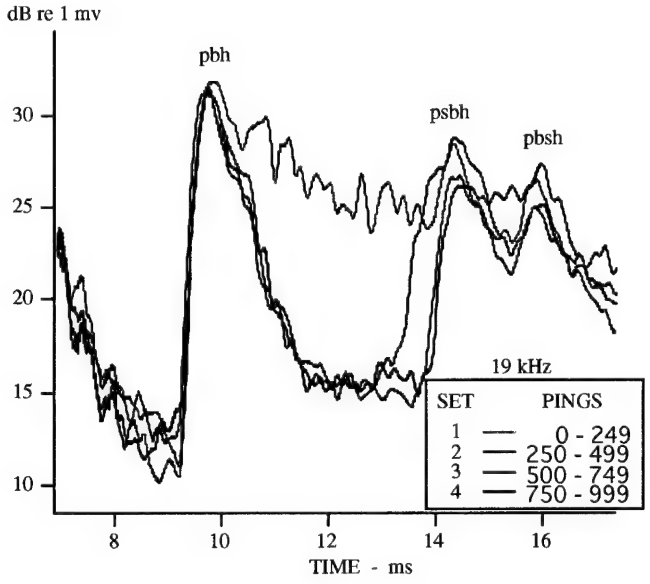

Figure 8 *Average signal intensities from the 4 sets of 250 pings at 19 kHz.*

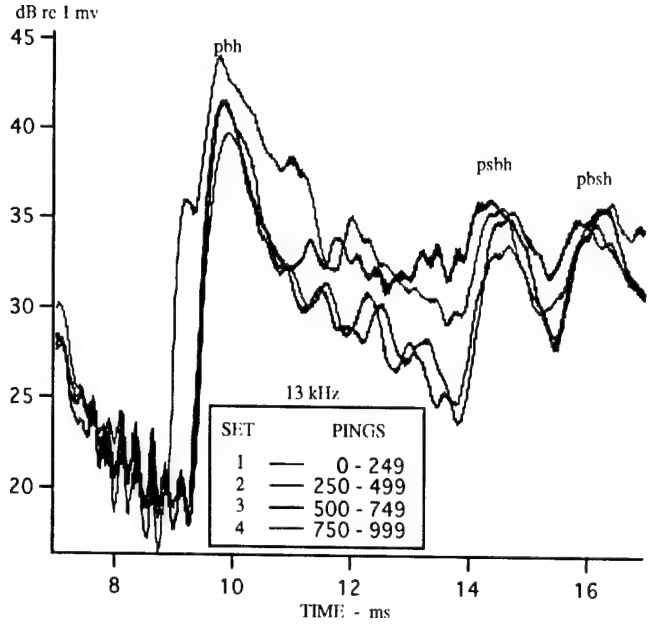

Figure 8 *Average signal intensities from the 4 sets of 250 pings at 13 kHz.*

For a truly stationary random process, the differences between the averages should be consistent with the estimated standard deviation at all time samples. In reality, this was not the case. The differences between averages were smallest at the peak of the direct path pulse (ph), at less than 0.01 dB, confirming the stability of the direct path signal. Regarding the direct path signal, small changes in the path length due to relative motion of projector and hydrophone caused changes in arrival time, which tended to increase the differences at time samples along the slopes on either side of the peak. The differences were less than 0.2 dB on the side preceding the peak, but reached as much as 4 dB on the trailing side, suggesting that, in addition to the arrival time perturbation, there was a significant volume reverberation contribution. Regarding the bottom reflection signal, the difference between averages were greater than the expected standard deviation at all points within the selected time window. The dominant cause is the vertical motion of projector and hydrophone assembly relative to the bottom, which could be several centimetres. The range and statistics of the vertical motion may vary from one group of pings to the next, depending on the surface conditions, causing the average shape of the peaks to differ significantly. Therefore, the averages, at each time sample, differed by a value considerably larger than the expected standard deviation.

The critical issue is the acoustic energy integral within the selected time windows. In the case of the direct path signal, the integrated energy differences were less than 0.1 dB, with most of the variations coming from the volume scattering in the decay tail. In the

case of the bottom reflection, the differences were consistent with the expected standard deviation of 0.27 dB - the largest measured was 0.6 dB.

4

Mean intensity profiles

To observe the average intensity profile as a function of frequency, the accepted signals were filtered in 2 kHz bands, centred at frequencies 1 kHz apart, starting at 8.5 and ending at 17.5 kHz. Each pass-band is a cosine tapered window (Fig. 10) 2 kHz wide at the half-amplitude (-6 dB) point. The 8.5 and 9.5 kHz bands were filtered from the pings that were generated by three cycles of a 9 kHz carrier, because the signal spectrum had continuous coverage from 6 to 11 kHz. The 10.5 and 11.5 kHz bands were filtered from the 11 kHz signal for similar reasons. The 15.5, 16.5 and 17.5 kHz bands were filtered from the 19 kHz signal, because its spectrum had continuous coverage from 13.5 to 19.5 kHz and also because all the 17 kHz data had been rejected. Higher frequency bands were not available because there was a low pass filter in the receiving circuitry that eliminated significant spectral components above 19.5 kHz.

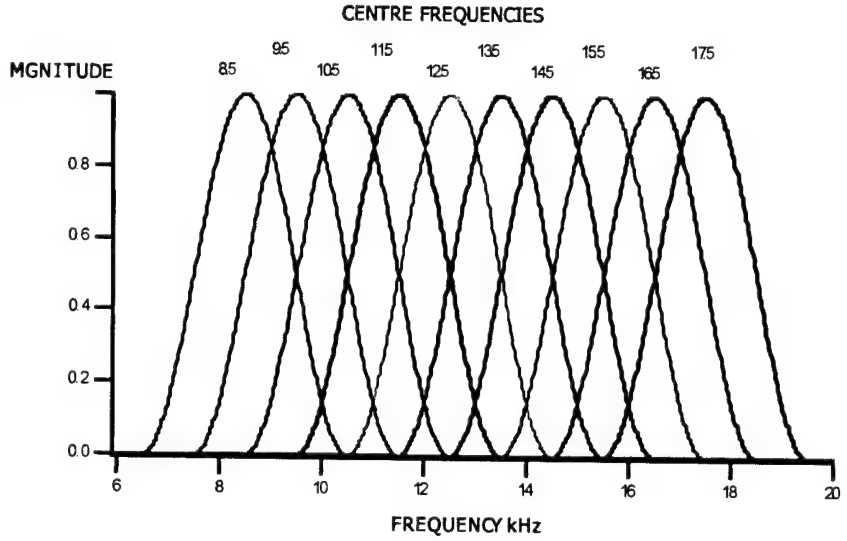

Figure 10 *Filter pass-bands.*

The filtered and averaged signal intensity profiles were normalized, by setting the peak of the direct path component to zero dB. The results are compared in Fig. 11. The main lobe of the direct path signal (ph) appears to be independent of frequency, which is expected,

since the bandwidths were identical. The differences appear to be in the subsequent decay tail. The 8.5 and 9.5 kHz signals have the largest decay tails, probably because the projector has a tendency to ring at these frequencies. The electrical feedover interference is also visible (e1).

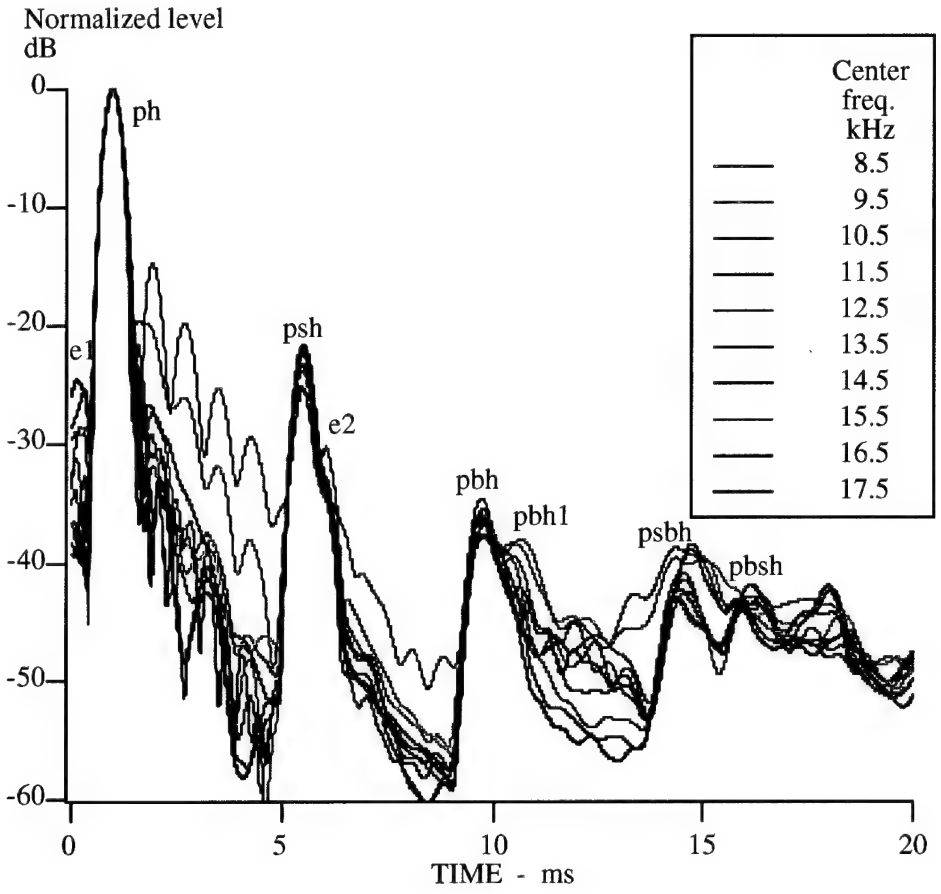

Figure 11 *Average intensity profiles in overlapping bands.*

The surface reflected signal (psh) is the next strongest feature. This is the signal that is launched from the back of the projector, bounced from the water-air surface and received by the hydrophone. The levels appear to be increasing with frequency, which probably reflects the frequency dependence of the front-to-back ratio of the projector. The shape of

its intensity profile is distorted due to the presence of an unwanted electrical interference pulse (e2).

The third feature is the bottom reflection signal (pbh). An expanded view of the bottom reflection profile is shown in Fig. 12. If the intensity level at the 9 ms mark may be used as an upper bound estimate of the background noise, then it appears that the bottom reflection peak is approximately 20 dB above the noise floor, except at 8.5 kHz where the ringing of the transducer has significantly raised the noise floor.

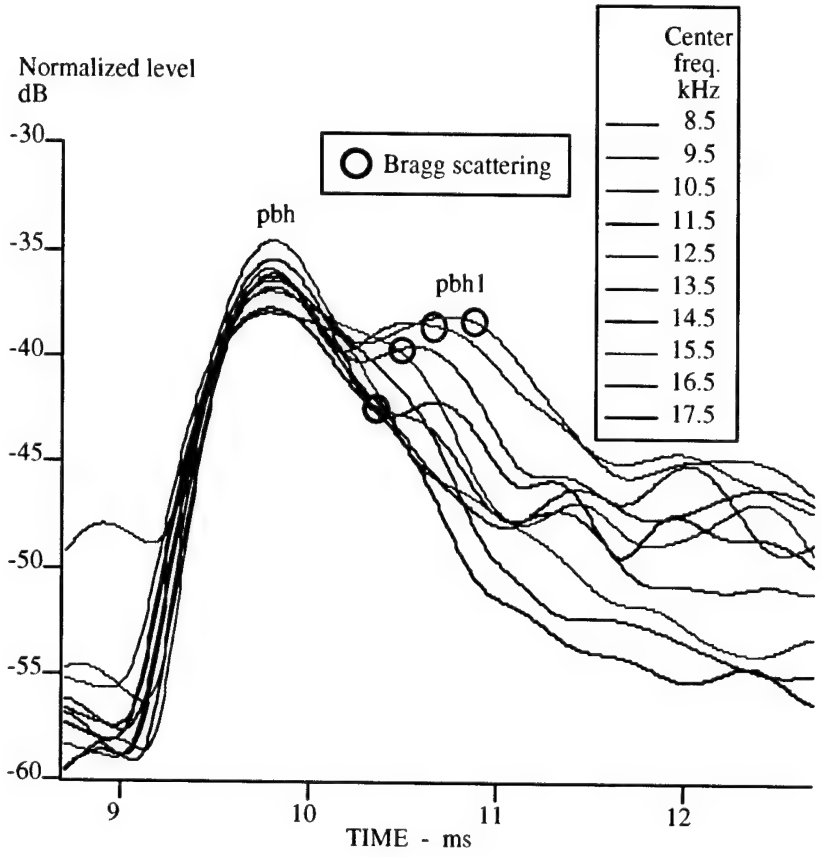

Figure 12 *Expanded view of the bottom reflected signal intensity profile.*

The signals at 8.5, 9.5, 10.5 and 11.5 kHz show a second peak, labeled "pbh1", which could be due to number of causes, the two most likely being: (1) one or more reflections from a sub-bottom layer, or (2) scattering from surface roughness. If it were the former,

the time delay would suggest that it came from a depth of approximately 0.7 m. Given that the attenuation of sound in sand is typically 0.5 dB per wavelength, the two-way attenuation loss at 8.5 kHz would be 4 dB. The sound level at the pbh1 peak is only 7 dB below that of pbh, therefore the reflection loss at the sub-bottom layer would have to be only 3 dB. This reflection loss is too low for an unconsolidated sediment layer. It would have had to be solid rock or a gas layer. At 17.5 kHz the two-way attenuation would be 8 dB, which is about 4 dB more than that at 8.5 kHz, therefore it should be detectable at all frequencies within the band, but in fact it is only detectable at the four lowest frequencies. For these reasons, the sub-bottom layer hypothesis was rejected.

If the peak at pbh1 were due to surface scattering, it should have some connection with the surface roughness spectrum of the sand, particularly the ripple structure. From the photograph in Fig. 6, it appears that the sand ripples are roughly 0.2 m apart. Given the height above bottom of the projector and receiver, it is possible to estimate the conditions for Bragg scattering. Constructive interference would occur when the scattered signal paths differ by an integral number (n) of wavelengths. At 8 kHz, this would occur at a range (R_n) of 3.46 m from the point directly beneath the transducers and the corresponding time delay (T_n) would be 1.08 ms relative to the normal incidence bottom reflection path, as illustrated in the Fig. 13. The corresponding values at the other signal frequencies are also shown. The time delay values (T_n) are also marked on the respective signals in Fig. 12. It is predicted that T_n would decrease with increasing frequency and this appears to be consistent with the data at the three lowest frequencies, 8.5, 9.5 and 10.5 kHz. At higher frequencies, T_n is expected to be so small that the Bragg peak would not be separable from the main arrival. Therefore, it is likely that the second and subsequent peaks are due to surface roughness scattering effects.

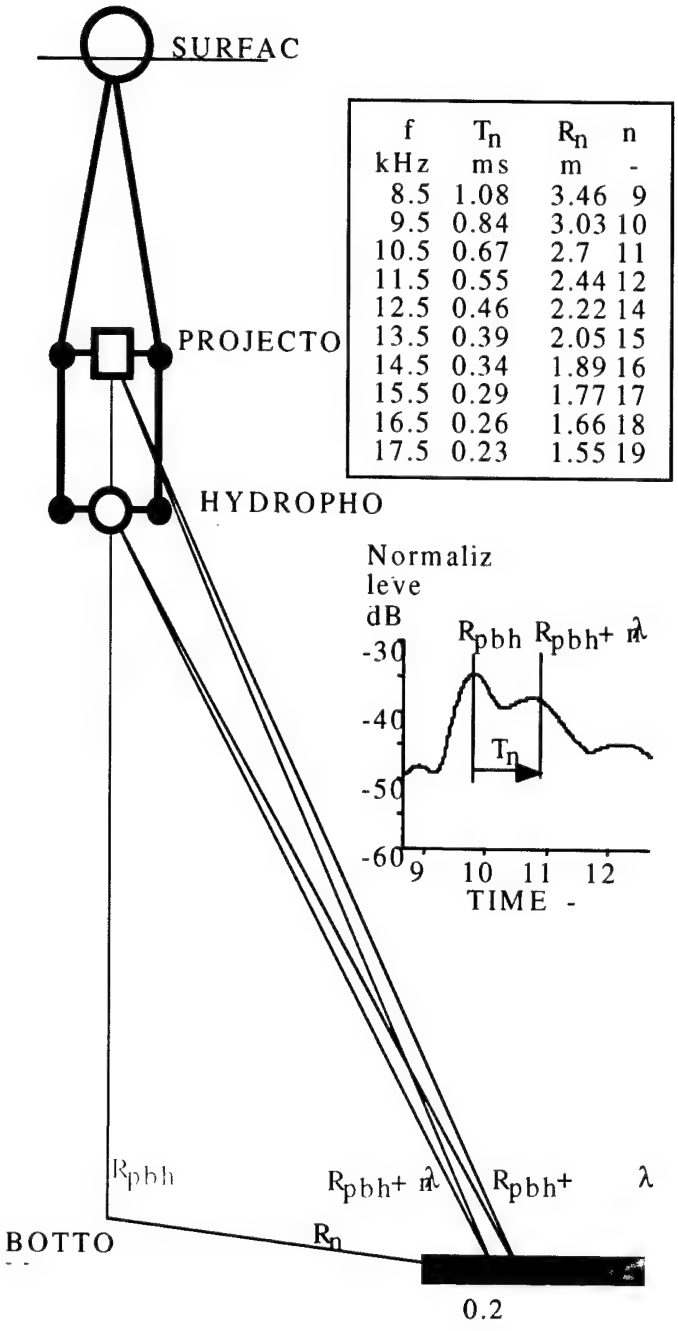

Figure 13 *Illustration of Bragg scattering by sediment surface ripples.*

5
Reflection loss computation

The concept of a reflection coefficient is a simple one. The reflection loss is the difference, in decibels, between the intensities of the incident and reflected waves. The magnitude of the reflection coefficient, in decibels, omitting the negative sign, is equal to the reflection loss.

In practice, the measurement is more complicated because the transducers were placed at some distance from the interface, the wave fronts were not planar and the water-sediment interface was not perfectly flat. The following steps were taken to mitigate these limitations. (1) Spreading and absorption loss corrections are used to compensate for the distances between the projector, hydrophone and interface. (2) The wave front curvature problem was reduced by placing the projector as far as practicable from the interface. For normal incidence, the water depth was a practical limitation. It was necessary to assume that the reflection coefficient changes insignificantly over the range of significant angles, i.e. the range of angles subtended by the significant Fresnel zones at the interface. Given the frequency band and height above bottom, the range of angles is approximately within $\pm 10°$ up to the third Fresnel zone. (3) There is a randomness in the reflected signal, which may be due in part to the surface roughness, but also to spatial variability of the reflection coefficient itself. This randomness precludes meaningful measurement of the complex reflection coefficient. However, by averaging the intensity of the incident and reflected signals, it is possible to obtain repeatable statistics. Using pulses, rather than continuous signals, the different signals were separable according to travel time. With reference to Fig. 11, it is evident that the pulse duration of the incident intensity (ph) is shorter than that of the averaged reflected signal (pbh). The time spreading of the reflected signal may be due to random changes in height above bottom of the transducers during the course of the experiment and scattering effects.

Given the above conditions, there are a number of ways that the reflection loss may be computed. Two were considered: (1) The reflection loss may be computed from the intensity difference measured at the peaks. In this case, the loss may be over estimated due to the time spreading of the reflected energy, which tends to suppress the peak of the averaged reflected intensity. (2) The reflection loss may be computed from the difference between the time integrals of the intensity pulse, i.e. the energy densities. This result would recapture most of the reduction in the peak value due to the time spreading, which was mainly caused by interface roughness. The resulting value may slightly underestimate the true reflection loss because the energy in the tail of the reflected signal pulse would probably include additional energy scattered from inhomogeneities within the volume beneath the sediment interface. On balance, method (2) is expected to be more accurate because the effect of time spreading due to bottom roughness is quite large, but the additional energy from volume scattering beneath the interface is expected to be relatively insignificant.

Using the intensity profiles in Fig. 11, both methods were used. The integration windows chosen were 0.4 to 4.4 ms for the direct signal and 9 to 13 ms for the bottom reflection. The window for the direct signal included the main peak and several range lobes of the direct path signal. The window for the bottom reflected signal included the main peak and the decay tail with all of its minor lobes, but excluding the multipath components psbh and pbsh. The decay tail was included because it is an integral part of the energy reflected from the bottom. Due to bottom roughness, some of the energy that would have been received, had the bottom been perfectly flat, was scattered out of the receiver path and lost, resulting in a reduction in the main peak. This is expected to be largely compensated by energy from surrounding areas scattered into the receiver path which shows up in the decay tail [5]. The spreading loss differences were estimated from the arrival times at the peaks (Fig. 14). With method (1), the reflection loss values were between 13 and 15 dB. Method (2) gave values between 9 and 13 dB. The latter values are considered to be the best estimates for the reasons given above.

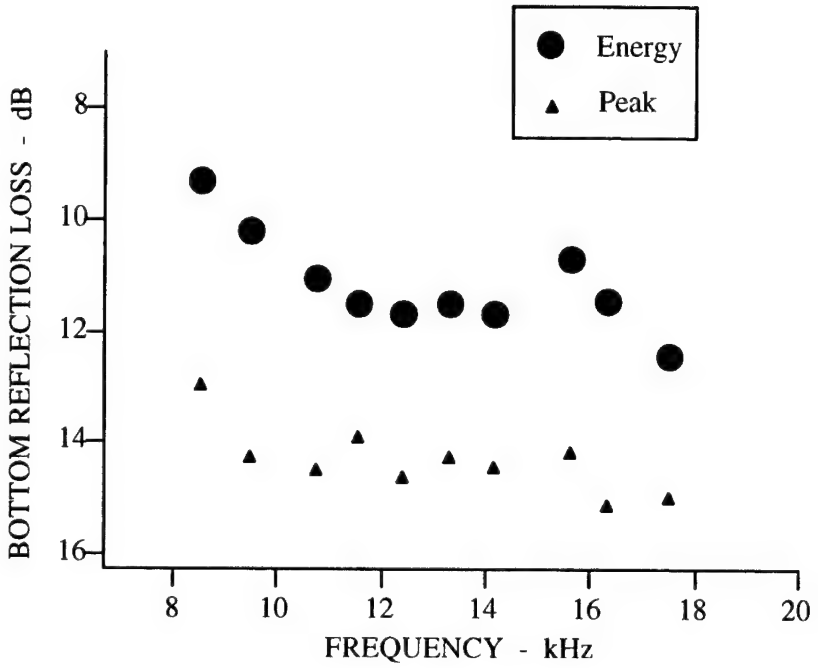

Figure 14 *Reflection loss as a function of frequency.*

The total measurement error E, in decibels, is composed of the following components, added logarithmically:

$$E = H + N + A \tag{1}$$

where H is the difference in the hydrophone receiving sensitivity between the upward and downward directions, N is the background noise contribution and A the contribution due to errors in transmission loss estimation.

As stated earlier, the variation in hydrophone sensitivity in the axial plane of the transducer was within +0.5 and – 1.5 dB. Accordingly, in subtracting the upward travelling reflected energy density, in decibels, from that of the downward travelling direct path, the error H due to hydrophone sensitivity variation cannot exceed 2 dB. From Fig. 11, the worst case noise floor, which is mainly due to transducer ringing, occurs at 8.5 kHz and it is approximately 13 dB below the average signal peak, both at ph and pbh. As a result, the peaks at ph and pbh are expected to be overestimated by 0.2 dB or less. Accordingly, the noise contribution, N, is estimated to be less than 0.2 dB. As the spherical spreading loss can be accurately computed from the pulse travel times, the contribution from transmission loss estimation is mainly due to the error in estimating the absorption loss. Allowing that the water temperature and salinity at the site were between 10°C and 15 °C and 30 and 35 ppt, the error, A, due to the uncertainty in absorption loss, according to the Francois and Garrison formula, is estimated to be less than 0.023 dB. Thus, the total measurement error, H + N + A, is expected to be less than 2.223 dB.

6
Conclusion

A self-calibrating method was used to measure the acoustic reflection loss at a water-sand interface, in which the same hydrophone is used to measure the incident and reflected signals. The results show reflection loss between 9 and 13 dB, consistent with reported values, *in situ* and in the laboratory (Fig. 15).

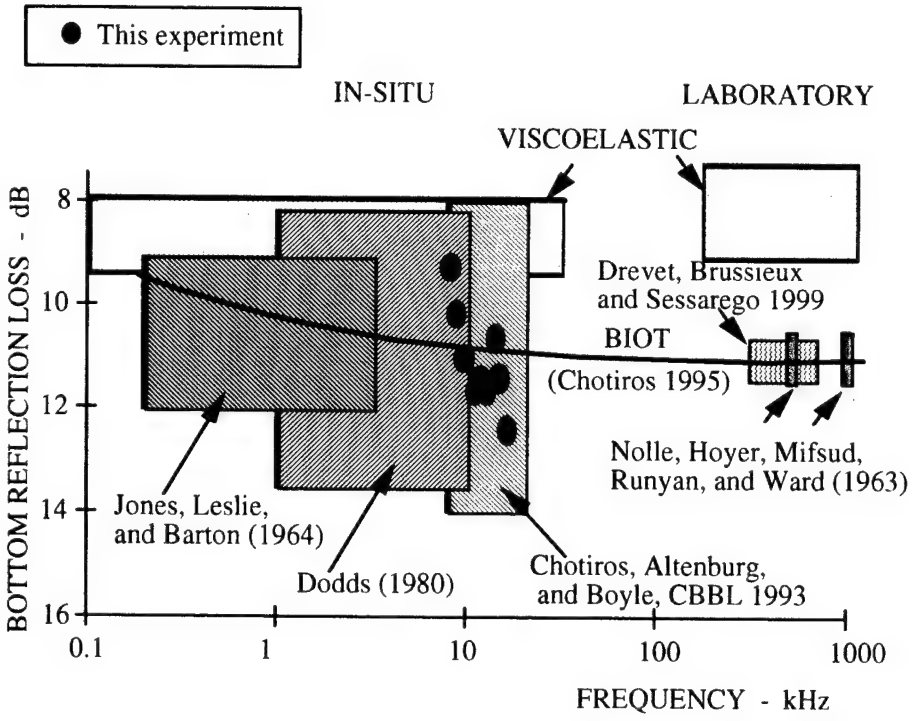

Figure 15 *Comparison with previous published measurements.*

It is instructive to examine the laboratory results before making concluding remarks about the *in situ* measurements. The laboratory measurements by Nolle, Hoyer, Mifsud, Runyan and Ward [7] were made at 500 kHz and 1 MHz, using graded, cleaned, degassed and packed sands: Four samples, with mean grain diameters, 0.64, 0.4, 0.17 and 0.12 mm, were used. The reflection loss was found to be 11 dB, with an error of ±0.5 dB, independent of grain size and frequency. The porosity and density of the water-saturated sand were 36% and 2069 kg/m^3, respectively and the sound speed ratio between sand and water was 1.16, independent of grain size. The density of the water was 1000 kg/m^3. The measured sound attenuation in the sand, a, in dB/m, was found to increase as the square root of frequency and inversely with grain diameter,

$$a = 0.016 \sqrt{f/d} \quad \text{dB/m}, \tag{2}$$

where f is frequency in Hertz and d is grain diameter in millimetres. The normal incidence reflection coefficient at the interface between two elastic media is simply given by the impedance ratio,

$$R_{elastic} = (z_s - z_w)/(z_s + z_w). \tag{3}$$

In the lossless case, the impedances of the sand and water, z_s and z_w, are simply equal to the product of the density and the sound speed. Given the above values, the elastic medium reflection coefficient was computed to be 0.41, which represents a reflection loss of 7.7 dB. Using a visco-elastic medium model, a similar calculation that takes account of the attenuation in the sediment gave the same value within a tenth of a decibel. Within the known range of values of the sound attenuation coefficient in sand, which is 1 decibel per wavelength or less at all relevant frequencies, it makes no difference if the visco-elastic medium is a causal model with one or more relaxation times or a non-causal model with a constant complex bulk modulus. The computed normal incidence reflection loss falls within a tenth of a decibel of the lossless case. If an allowance of 5% is made for the accuracy of the measured density and sound speed, the predicted values range from 7.2 to 9.1 dB. Clearly there is a discrepancy between the measured and theoretical values. This result is consistent with a similar laboratory measurement by Drevet, Brussieux and Sessarego [8] in the frequency band 300 - 700 kHz.

The measurements by Dodds [9] and Jones, Leslie and L. E. Barton [10] were made *in situ*, but there was little environmental information to describe the sediment other than that it was sand. In situ measurements by Chotiros, Altenburg and Boyle [11,12] over a sandy sediment, near Panama City, Florida, in 1993, under the Coastal Benthic Boundary Layer (CBBL) program, were supported by extensive environmental measurements [13]. The measured values of sediment density and sound speed ranged from 1907 to 2096 kg/m^3 and 1650 to 1750 m/s, respectively. The sound speed was measured in core samples at 400 kHz. The corresponding parameter values for the water above the sediment were 1020 kg/m^3 and 1530 m/s, respectively. Using these values, the reflection loss was computed to be between 7.9 and 9.4 dB. The theoretical and measured values are compared in Fig. 15. Although there is some overlap between the predicted and

measured range of values, there is clearly a discrepancy that cannot be entirely explained as experimental error.

The elastic parameters associated with the data reported here are very similar to those of Chotiros, Altenburg and Boyle, with one exception. The acoustic measurements by Maguer, Fox, Schmidt, Pouliquen and Bovio [6] suggested that there was significant dispersion, specifically that the sound speed measured at 200 kHz may be higher than that at the lower frequencies where the reflection measurements were made. They deduced from propagation measurements that the sediment sound speed in the frequency range 2 - 15 kHz was 1685 m/s instead of the 1720 m/s measured from cores at 200 kHz. These values still fall within same the range of sound speed values as the Chotiros, Altenburg and Boyle data and therefore the same range of computed visco-elastic reflection loss values would be applicable. The measured values are consistent with the values from the Chotiros, Altenburg and Boyle data, but with a smaller spread about the mean value. The data points are plotted as ovals in which the vertical extent represents the expected one standard deviation excursion of ±0.27 dB and the horizontal extent covers the bandwidth. All but one data point fell outside the expected range of reflection loss values predicted by the visco-elastic model. The remaining variations in the measured values are probably due to variations in the front-to-back ratio of the hydrophone sensitivity as a function of frequency and are unlikely to contain useful information about the frequency dependence of the sediment properties.

In all known cases, the measured reflection loss at normal incidence is inconsistent with the visco-elastic media model above and beyond expected errors in six independent experiments, two in the laboratory and four *in situ*, in the band from 1 kHz to 1 MHz. The experiment reported herein is particularly reliable due to the self-calibration approach adopted. As sand is a porous medium rather than a uniform elastic solid, Biot's model [3,4] of sound propagation in a porous elastic medium is likely to be a better alternative. One notable difference between the visco- and poro-elastic models is that the latter specifies two compressional waves. The second wave, though rarely observed, readily absorbs energy and would account for the enhanced reflection loss. Using parameters for sand put forward by Chotiros [14], good agreement with the measured values are obtained, as shown in Fig. 15. This computation can be accomplished with readily available computer programs from various sources, including BOGGART3 from N. P. Chotiros, at ARL:UT and OASES 2.1 from H. Schmidt, at MIT. However, more recent publications [15,16] suggest that aspects of this model, specifically the procedure for estimating certain input parameter values used by Chotiros [14] and the constitutive equations in Stoll and Kan [4], are not entirely satisfactory and more research is needed to establish a physically sound model for sandy sediments.

In conclusion, the Biot model is put forward as a candidate solution for two reasons. (1) It has a loss mechanism, i.e. the slow wave, that can account for a reflection loss in excess of what the visco-elastic model can accommodate. (2) There is a tentative set of parameter values [14] which is consistent with the measured values of reflection loss, wave speed and attenuation, as well as the known geophysical properties. For these reasons, the Biot model represents a step forward in our understanding of the underlying physical processes in the acoustics of water-saturated sand.

7 Acknowledgements

The experiment was conducted by SACLANTCEN as part of the Acoustic Penetration Experiment (APEx). Thanks are due to the commander and crew of the Research Vessel *Manning* and the SACLANTCEN engineering staff who provided excellent support. The analysis of the reflection data was funded by the Office of Naval Research Code 321 OA, under the Broad-band High-Frequency Sound Interaction with the Sea Floor Program, under the management of Dr. Jeff Simmen.

References

[1] Heard, G.J. Bottom reflection coefficient measurement and geoacoustic inversion at the continental margin near Vancouver Island with the aid of spiking filters. *Journal of the Acoustical Society of America,* **101,** 1997:1953-1960.

[2] Hamilton, E.L. Reflection coefficients and bottom losses at normal incidence computed from pacific sediment properties. *Journal of the Acoustical Society of America,* **35**, 1970:995-1004.

[3] Biot, M.A., Willis, D.G. The elastic coefficients of the theory of consolidation. *Journal of Applied Mechanics*, **24**, 1957:594-601.

[4] Stoll, R. D., Kan, T.K. Reflection of acoustic waves at a water-sediment interface. *Journal of the Acoustical Society of America,* **70**, 1981:149-156.

[5] Chotiros, N.P. Reflection and reverberaton in normal incidence echo-sounding. *Journal of the Acoustical Society of America,* **96**, 1994:2921-9.

[6] Maguer, A., Fox, W.L.J., Schmidt, H., Pouliquen, E., Bovio, E. Mechanisms for subcritical penetration into a sandy bottom: Experimental and modeling results. *Journal of the Acoustical Society of America,* **107**, 2000:1215-1225.

[7] Nolle, A.W., Hoyer, W.A., Mifsud, J.F., Runyan, W.R., Ward, M.B. Acoustical properties of water- filled sands. *Journal of the Acoustical Society of America,* **35**, 1963:1394-1408.

[8] Drevet, C., Brussieux, M., Sessarego, J. P. High frequency acoustic wave reflection on the surf zone seafloor, *Acustica*, No. 5, 1999:701-706.

[9] Dodds, D.J. Attenuation estimates from high resolution subbottom profiler echoes. Kuperman, W.A., Jensen, F.B. (editors). *Bottom-Interacting Ocean Acoustics,* 525-540, NATO Conference Series IV; Marine Sciences, Plenum Press, New York, (1980).

[10] Jones, J.L., Leslie, C.B., Barton, L.E. Acoustic characteristics of underwater bottoms. *Journal of the Acoustical Society of America,* **36**, 1964:154-7.

[11] Chotiros, N.P., Altenburg, R.A., Boyle, F.A. Reflection coefficient of sandy ocean sediments in shallow water, *EOS*, **75**, 1994:181.

[12] Chotiros, N.P. Inversion and sandy ocean sediments. *In*: Diachok, O., Caiti, A., Gerstoft, P., Schmidt, H. *editors*. Full Field Inversion Methods in Ocean and Seismic Acoustics, Kluwer Academic Press, 1995. [ISBN 0-7923-3459-0].

[13] Richardson, M.D., Griffin, S.R. *In situ* sediment geoacoustic properties. Coastal Benthic Boundary Layer Special Research Program: First Year, Report No. NRL/MR/7431-94-7099, Michael D. Richardson Ed., pp. 146 - 148, Stennis Space Center, MS, Naval Research Laboratory, 1994.

[14] Chotiros, N.P. Biot model of sound propagation in water-saturated sand. *Journal of the Acoustical Society of America,* **97**, 1995:199-214.

[15] Stoll, R.D. Comments on Biot model of sound propagation in water-saturated sand [*Journal of the Acoustical Society of America,* 97, 199-214 (1995)]. *Journal of the Acoustical Society of America,* 103(5), Pt. 1, 2723-2725, (1998).

[16] Briggs, K.B., Richardson, M.D., Williams, K., Thorsos, E.I. Measurement of grain bulk modulus using sound speed measurements through liquid/grain suspensions. *Journal of the Acoustical Society of America,* **104**, 1999:1788.

Document Data Sheet

Security Classification		Project No.
UNCLASSIFIED		03-D
Document Serial No.	**Date of Issue**	**Total Pages**
SR-335	July 2001	30 pp.

Author(s)

.Chotiros, N.P., Lyons, A.P., Osler, J., Pace, N.G.

Title

Normal incidence reflection loss from a sandy sediment

Abstract

Acoustic reflection loss at normal incidence of a sandy sediment, in the Biodola Gulf on the north side of the island of Elba, Italy, was measured in the band 8 - 17 kHz, using a self-calibrating method. The water depth was approximately 11 m the sand pure with a mean grain diameter of 0.2 mm. The measured reflection loss 11 dB, ±2 dB is consistent with measurements in the published literature. The computed reflection loss for an interface between water and a uniform visco-elastic media with the same properties was 8 dB, ±1dB. The theoretical and experimental values do not significantly overlap, which leads to the conclusion that the visco-elastic model is inappropriate. The Biot model is suggested as a better alternative but more work is needed to ascertain the appropriate parameter values.

Keywords

Acoustic reflection loss - Biot model - seafloor sediments

Issuing Organization

North Atlantic Treaty Organization
SACLANT Undersea Research Centre
Viale San Bartolomeo 400, 19138 La Spezia, Italy

[From N. America: SACLANTCEN (New York) APO AE 09613]

Tel: +39 0187 527 361
Fax:+39 0187 527 700

E-mail: library@saclantc.nato.int

The SACLANT Undersea Research Centre provides the Supreme Allied Commander Atlantic (SACLANT) with scientific and technical assistance under the terms of its NATO charter, which entered into force on 1 February 1963. Without prejudice to this main task - and under the policy direction of SACLANT - the Centre also renders scientific and technical assistance to the individual NATO nations.

This document is approved for public release.
Distribution is unlimited

SACLANT Undersea Research Centre
Viale San Bartolomeo 400
19138 San Bartolomeo (SP), Italy

tel: +39 0187 527 (1) or extension
fax: +39 0187 527 700

e-mail: library@saclantc.nato.int

NORTH ATLANTIC TREATY ORGANIZATION